Possibilities of subunit localization with fluorescent protein tags and electron microscopy examplified by a cyanobacterial NDH-1 study

Birungi, Mariam; Folea, Mihaela; Battchikova, Natalia; Xu, Min; Mi, Hualing; Ogawa, Teruo; Aro, Eva-Mari; Boekema, Egbert J.

Published in:
Biochimica et Biophysica Acta-Bioenergetics

DOI:
10.1016/j.bbabio.2010.06.004

Publication date:
2010

Biochimica et Biophysica Acta 1797 (2010) 1681–1686

Contents lists available at ScienceDirect

Biochimica et Biophysica Acta

journal homepage: www.elsevier.com/locate/bbabio

Possibilities of subunit localization with fluorescent protein tags and electron microscopy examplified by a cyanobacterial NDH-1 study

Mariam Birungi [a], Mihaela Folea [a], Natalia Battchikova [b], Min Xu [c], Hualing Mi [c], Teruo Ogawa [c], Eva-Mari Aro [b], Egbert J. Boekema [a,*]

[a] Groningen Biomolecular Sciences and Biotechnology Institute, University of Groningen, Nijenborgh 4, 9747 AG Groningen, The Netherlands
[b] Department of Biochemistry and Food Chemistry, University of Turku, FIN-20014 Turku, Finland
[c] Shanghai Institute of Plant Physiology and Ecology, Shanghai, 200032, China

ARTICLE INFO

Article history:
Received 23 April 2010
Received in revised form 1 June 2010
Accepted 7 June 2010
Available online 12 June 2010

Keywords:
NDH-1
Electron microscopy
Subunit labeling
Yellow fluorescent protein
Synechocystis 6803

ABSTRACT

Cyanobacterial NDH-1 is a multisubunit complex involved in proton translocation, cyclic electron flow around photosystem I and CO_2 uptake. The function and location of several of its small subunits are unknown. In this work, the location of the small subunits NdhL, -M, -N, -O and CupS of *Synechocystis* 6803 NDH-1 was established by electron microscopy (EM) and single particle analysis. To perform this, the subunits were enlarged by fusion with the YFP protein. After classification of projections, the position of the YFP tag was revealed; all five subunits are integrated in the membrane domain. The results on NDH-1 demonstrate that a GFP tag can be revealed after data processing of EM data sets of moderate size, thus showing that this way of labeling is a fast and reliable way for subunit mapping in multisubunit complexes after partial purification.

1. Introduction

There is nowadays a strong call for tools to localize specific proteins or protein subunits within cells or subcellular components. Light microscopy can fulfill this demand on the level of cells, but not at high resolution within subcellular compartments or macromolecules. In the last decades antibody-labeling has been one of the most widely applied techniques in cell biology, often in combination with thin sectioning and electron microscopy. This allows to directly localize specific proteins in cell sections, because small gold clusters, linked to the antibodies raised against these proteins, can be easily visualized. Antibodies can also be used to localize proteins within large multisubunit protein complexes. A typical example is the early work on mapping ribosomal subunits by Georg Stöffler and colleagues [1]. This immuno-mapping method is, however, elaborative and time consuming.

On the lower resolution cellular level, light microscopy has gained a lot of impact from genetic labeling with green fluorescent protein (GFP) and its homologs as fluorescent tags [2,3]. GFP and related proteins are stable β-barrel proteins that allow for the visualization of dynamic processes in living cells. The use of GFP-fusion proteins has facilitated the study of the distribution and movements of proteins in cells without the use of secondary reagents. They have also been applied for the subcellular localization of proteins by electron microscopy [4]. Because of their fluorescent capacity, GFP-fusion proteins are also useful in biochemical investigations, for instance to follow protein assembly and insertion into multisubunit protein complexes, such as human mitochondrial complex I. By using six GFP-tagged subunits a stepwise assembly process of complex I involving pre-assembled modules could be established [5]. Surprisingly, the popular GFP-fusion products have hardly been tried out to localize protein subunits on the level of multiprotein complexes, as will be the topic of this paper.

Complex I (NADH: Ubiquinone oxidoreductase) in mammalian mitochondria consists of not less than 45 different subunits (see [6] for a recent review). Nevertheless, it shares similarity to the much smaller prokaryotic complex I/NDH-1 enzymes, because the eukaryotic and prokaryotic complexes have a set of 14 core subunits in common [7]. In prokaryotes there is a little variation in the set of 14 core subunits; some species like *Escherichia coli* have only 13 subunits because two genes have been fused [8], whereas others have additional unique subunits, like *Thermus thermophilus* [9]. The cyanobacterial NDH-1 and the chloroplast NDH complex differ from those of non-photosynthetic organisms such as *E. coli* in the lack of genes encoding for three hydrophilic, water-soluble subunits named NuoE, -F and -G with dehydrogenase activity [10]. Instead, they are comprised of additional unique subunits. Further, a specific difference with *E. coli* complex I is a heterogeneity derived from variations in subunit composition. NDH-1L and NDH-1MS are two variants of NDH-1, differing in the NdhD and -F subunits in the membrane (see [10] for more details).

The chloroplast NDH complex and the cyanobacterial NDH-1L complex are close relatives and have fifteen homologous subunits,

* Corresponding author. Tel.: +31 50 3634225; fax: +31 50 363 4800.
E-mail address: e.j.boekema@rug.nl (E.J. Boekema).

0005-2728/$ – see front matter © 2010 Elsevier B.V. All rights reserved.
doi:10.1016/j.bbabio.2010.06.004

including NdhL, -M, -N and -O which are specific for photosynthetic organisms [11–14]. The chloroplast NDH complex has several recently discovered additional subunits [13,14,15–18], whereas the cyanobacterial NDH-1MS complex has the unique CupA and CupS subunits involved in carbon acquisition [19–21]. CupA is involved in CO_2 acquisition and loosely attached to the tip of the membrane domain of the NDH-1MS complex [28]. At present it is not clear what roles CupS and the subunits NdhM, -N, -L and -O play in the cyanobacterial complex and where they are located. CupS and the NdhM, -N and -O subunits are considered to be water soluble, while the NdhL subunit has two transmembrane domains. Its chloroplast ortholog CRR23 has three membrane spanning domains and CRR23 has been found to be essential for stabilizing the NDH complex in chloroplasts [14].

There is no high-resolution structure available for a complete Complex I or NDH-1 complex. However, the structure of the hydrophilic domain from *Thermus thermophilus* Complex I was solved by X-ray diffraction at 3.3 Å resolution [22] and shows the unique chain of iron–sulfur clusters. In addition, many low-resolution structures of Complex I and NDH-1 have been provided by electron microscopy, and they all show the special L-shaped form of these enzymes [24–26], but lack to reveal the details of the proton pump. The cyanobacterial NDH-1 complex resembles in size and shape the other eukaryotic and prokaryotic complex I enzymes, which have an overall L-shaped form, consisting of a membrane domain and a peripheral, hydrophilic domain, which is further divided into 6 structural domains in *Y. lipolytica* and bovine complex I [24]. The main difference of cyanobacterial NDH-1 with these complex I particles and *E. coli* complex I is the lack of the above mentioned NuoE, -F, -G subunits. The lack of cyanobacterial counterparts of the NuoE, -F, -G subunits leads to the absence of the domains 1 and 2, as resolved in the *Y. lipolytica* and bovine complex I structures [24].

Over the last two decades, single particle electron microscopy (EM) has provided hundreds of 2D and 3D structures of large protein complexes, ribosomes and viruses. In favorable cases, such as the rigid and highly symmetrical virus molecules, single particle EM has provided near-atomic resolution [27], allowing to fit amino acids in a way which is common practice in X-ray diffraction. By single particle averaging it is possible to easily detect a protein tag if its mass is about 10 kDa or larger. GFP and YFP, with a mass of 27 kDa, meet this criterion and thus allows to map the underlying subunit positions with an accuracy of about 20 Å. GFP was first applied for structural analysis of the cardiac ryanodine receptor type 2, which is a homotetramer [27]. Three-dimensional reconstruction of RyRs has provided information about the organization of the internal domains but the best resolution to date (10 Å) is still too low to unambiguously reveal the organization and boundaries of the subunits. EM and single particle image processing of a GFP-fusion protein revealed the location of the inserted GFP in a specific domain within a 3D reconstruction of the mutated protein [27]. In this paper we have addressed the location of the small subunits NdhL, -M, -N, -O and CupS in *Synechocystis* 6803 NDH-1 complexes. To this end, the subunits were enlarged by fusion with the YFP protein, which forms a stable β-barrel structure detectable by electron microscopy.

2. Materials and methods

2.1. Construction of Ndh–YFP fusion protein mutants

The *p*EYFP-6His-Sp^R plasmid was constructed using *p*EYFP vector (Clontech Laboratories, Inc. CA, USA), as illustrated in Fig. 1. The double stranded DNA containing *Bsr*G1 and *Not*I sites was obtained by annealing the following oligonucleotides synthesized chemically and was replaced with a small fragment cut out from *p*EYFP vector to create *p*EYFP-6His.

5′-GTACAAG$(CAT)_6$TAAAGC-3′
5′-CGGCCCGCTTTA$(ATG)_6$CTT-3′

The apectynomycin-resistant cassette was then inserted into NotI site of the vector to create *p*EYFP-6His-Sp^R. Six Ndh subunits, NdhL, -M, -N, -O, -E and CupS, were chosen for C-terminal YFP fusion. Corresponding genomic regions encoding these subunits and their downstream regions were amplified by PCR using primers with specific restriction sites and were ligated to *p*EYFP-6His-Sp^R into final constructs (Fig. 1 shows the construction of NdhL-YFP-6His), which were used to transform WT *Synechocystis* PCC 6803 to create mutants. Accuracy of plasmid assemblies was verified by sequencing.

2.2. Cultivation of cyanobacteria and preparation of Thylakoid membranes

Synechocystis sp. PCC 6803 WT and mutants containing Ndh subunits fused with YFP-6His were grown in BG-11 medium containing 20 mM

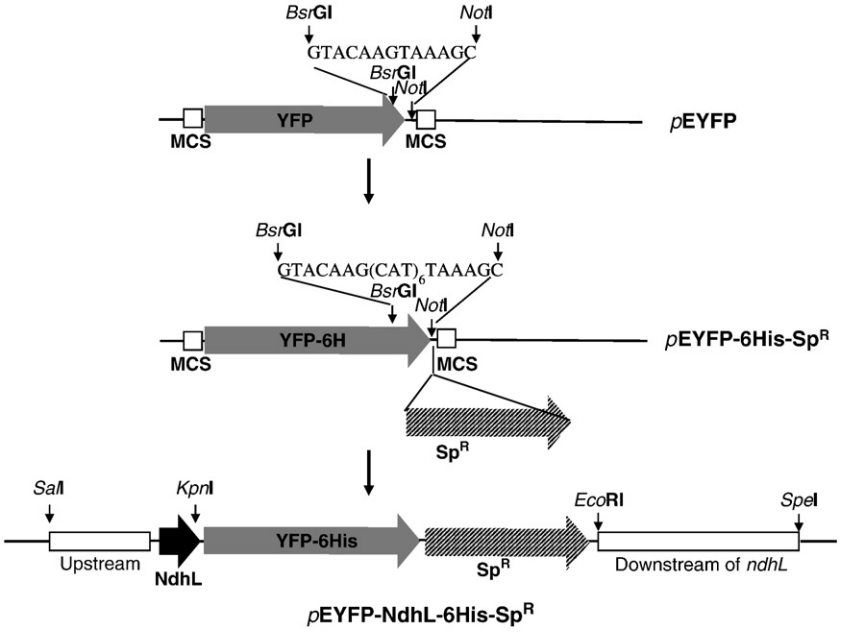

Fig. 1. Scheme for the construction of pEYFP-6His-Sp^R plasmid and its use for the production of NdhL-YFP fusion protein mutants.

HEPES, pH 7.5 under continuous light of 50 μmol photons m^{-2} s^{-1} at air level of CO_2. The thylakoid membranes of *Synechocystis* WT and mutant strains were isolated from 100 ml cell culture according to [20].

2.3. hrCN-PAGE analysis of membrane protein complexes

Thylakoid membranes were solubilized in a buffer containing 25 mM Bis–Tris, pH 7.5, 20% glycerol and 1.5% DM, for 30 min at +4 °C, centrifuged and the protein complexes were separated by 4.5–9% gradient hrCN-PAGE [29]. Gels were run at 50 V for 30 min, 75 V 30 min, 100 V 1 h and further at 200 V. Unstained gels were photographed and the YFP fluorescence of the thylakoid protein complexes was recorded by Geliance 1000 Imaging System (Perkin Elmer, UK). Fluorescence was excited with light <500 nm obtained with the low-pass filter LS500S (Corion Corp., MA), and the fluorescence emission was detected in the range of 550–600 nm (the SyberGold filter, Geliance 1000 Imaging System, Perkin Elmer, UK).

2.4. Preparation of Synechocystis 6803 membranes for electron microscopy

Thylakoid membrane samples from *Synechocystis* WT and mutants were solubilized at 0.4 mg/ml chlorophyll with 2% digitonin (final concentration) in buffer A (50 mM Tricine–NaOH pH 7.5, 30 mM $CaCl_2$) by stirring on ice for 2 h. Non-solubilized material was removed by centrifugation (14,000 rpm, 10 min) and the supernatant was loaded on a Ni^{2+}-NTA column. The column was washed with buffer A plus 0.2% digitonin and 10 mM imidazole and bound material was eluted with buffer A containing 0.2% digitonin and 160 mM imidazole.

2.5. Electron microscopy and single particle analysis

Affinity-purified samples were prepared for transmission electron microscopy by dilution in buffer A with detergent and subsequent negative staining using 2% uranyl acetate on glow-discharged carbon-coated copper grids. Electron microscopy was performed on a Philips CM120 equipped with a LaB_6 tip operating at 120 kV. The "GRACE" system for semi-automated specimen selection and data acquisition [30] was used to record 2048 × 2048 pixel images at 66,850× calibrated magnification (3.75 Å) with a Gatan 4000 SP 4 K slow-scan CCD camera. A total of 15,000 particle projections were collected. Single particle analysis was performed using Groningen Image Processing ("GRIP") software packages on a PC cluster. The best 70–80% of the class members was taken for the final class-sums.

3. Results

3.1. Verification of the presence of the Ndh–YFP fusion proteins NDH-1 complexes

To verify the successful incorporation of Ndh–YFP constructs to the NDH-1 complexes, the thylakoid protein complexes were solubilised by 1.5% DM and the protein complexes were separated by hrCN-PAGE. As shown in Fig. 2, two major fluorescent bands between the photosystem I trimer complexes and the band composed of photosystem I and photosystem II monomers were detected in the NdhL, -M, -N, -O and -E YFP-fusion mutants. These bands have earlier been identified as NDH-1L and NDH-1M complexes [20] thus demonstrating the incorporation of the Ndh–YFP constructs to the respective protein complexes. CupS-YFP mutant lacked the fluorescence from these two bands but emitted fluorescence at a lower molecular mass region where the NDH-1S complex was previously shown to migrate [20].

3.2. Analysis of YFP-tagged NDH-1 complexes

Because of the unique L-shape of cyanobacterial NDH-1 particles it is possible to detect their projections in negatively stained EM samples without a purification step [28]. Such samples contain a complete set of solubilized thylakoid membrane proteins, of which photosystem I and II, ATP synthase and NDH-1 are the largest ones [31]. In a previous investigation we used affinity chromatography for purification [25]. It was later found that this step easily removes the CupA subunit [28]. On the other hand, without any purification the numbers of NDH-1 particles per image are much lower. Therefore, an affinity purification step was applied prior to EM specimen preparation, but specimens were prepared within minutes after the chromatography step, in contrast to previous experiments where samples were stored frozen. The purification step did not yield pure samples, but they were highly enriched in intact complexes (Fig. 3), with at least about 10 good NDH-1 particle projections per image for all types of particles investigated, and on many particles the CupA subunit was still present at the tip of the membrane arm (Fig. 3).

3.3. Image processing of YFP-tagged NDH-1 complexes

Affinity-purified samples of the 6 mutants of NDH-1 complex with fused YFP labels were studied by electron microscopy. For 5 different subunits data sets of over 1000 identifiable NDH-1 particles in side-view position could be collected (yellow boxes, Fig. 3). The NdhE-YFP mutant did not give sufficient numbers of intact complexes upon

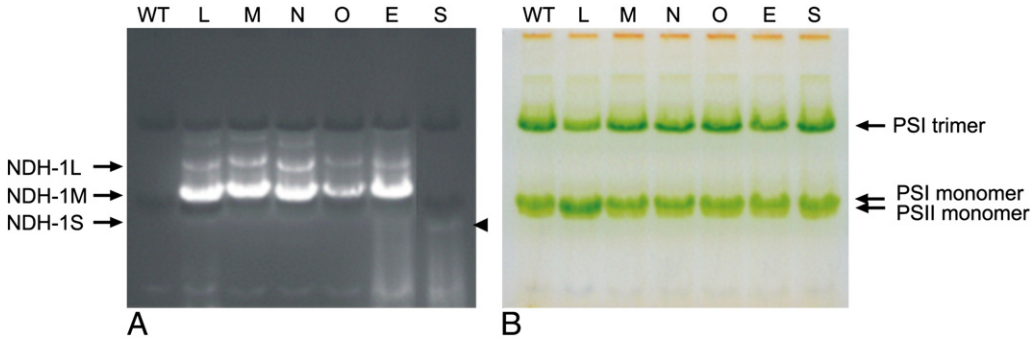

Fig. 2. Incorporation of YFP-fused Ndh subunits into NDH-1 complexes. Thylakoid membranes of WT and mutant *Synechocystis* cells were solubilized with 1.5% DM and analyzed by 4.5–9% gradient high-resolution clear native PAGE (hrCN-PAGE). A — Fluorescence of NDH-1 complexes with YFP-fused Ndh subunits. Arrows show positions of the NDH-1L complex and subcomplexes of the NDH-1MS complex, NDH-1M and NDH-1S (hrCN-PAGE dissociates the NDH-1MS complex into two subcomplexes [10], in contrast to affinity purification, used in the EM analysis). YFP-fused subunits NdhL, -M, -N, -O, and -E (lanes L, M, N, O, E, respectively) are present in NDH-1L and NDH-1M while the CupS-YFP protein is present in the NDH-1S complex (weak fluorescence marked by arrowhead). B — a photograph of the gel. Green bands correspond to chlorophyll-containing photosystem I and photosystem II complexes.

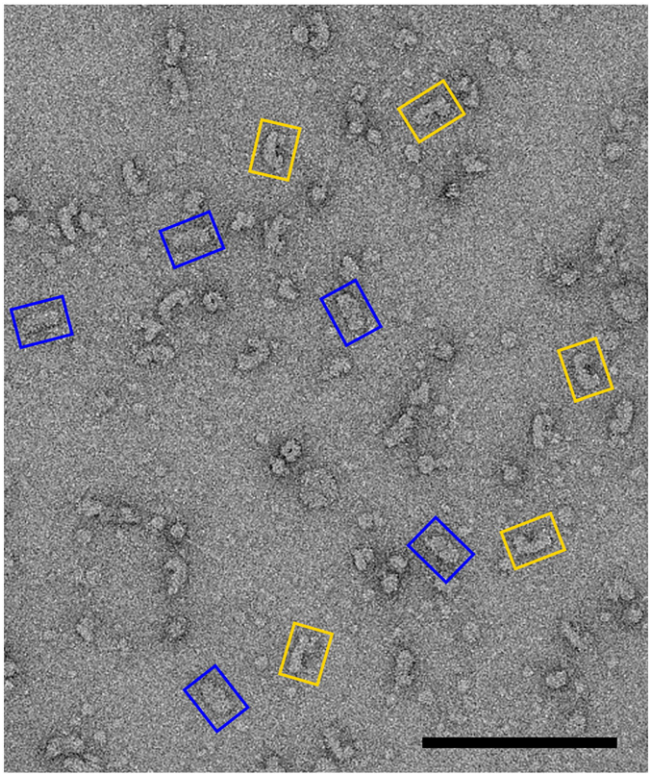

Fig. 3. Electron microscopy image of a negatively stained preparation of the NdhN-YFP-6His mutant after purification by Ni^{2+} affinity chromatography. Some side-view projections of NDH-1 complexes with the YFP tag on NdhN (yellow boxes), as well as top-view projections are indicated (blue boxes). Some of the side views are clearly U-shaped, indicating the presence of the CupA subunit. The scale bar is 100 nm.

solubilization and was not further considered. Also, top views were not selected because in these particular projections the large hydrophilic domain is fully overlapping with the membrane domain (blue boxes, Fig. 3). The ratio between top and side views was, however, about 1:1 in most samples.

All sets of selected single particle projections were separately analyzed by single particle averaging, which includes classification of projections and subsequent averaging of class members of homogenous subsets of particles ("classes") into 2D maps. The largest set of 6700 projections was collected for the subunit NdhN-YFP mutant and the classification showed the specific variation in the data set. The projections appeared to arise from particles in two different positions, resulting from a difference in attachment to the support film (left- and right-handedness, Fig. 4A,B versus 4C,D). In addition, the presence of the CupA domain at the tip of the membrane domain is variable, as observed before [24], because NDH-1 is a heterogenous complex, consisting of NDH-1L and NDH-1MS particles, of which only the latter has CupA bound. It is mostly or fully lacking in two classes (Fig. 4A,D), comprising 33% of the total set, just as it was observed in an analysis of NDH-1 of some years ago (Fig. 4O, [25]). Most importantly, an extra density, not observed before, is present in the middle of the membrane arm in three classes (red arrow, Fig. 4A,C,D). It is, however, fully lacking in the largest class of Fig. 4B and is present in 30% of the data set (Table 1). This extra density was not observed in previous studies and is therefore considered to be the YFP tag, also because of its size. There is clearly a correlation between its presence or absence and the occurrence of the CupA domain. The presence is clearly lower if the CupA domain is present (Fig. 4B). Finally, the NdhN-YFP data set showed variation in the hydrophilic domain; an extension of this domain was present in a small number (2%) of the particles (green arrowhead, Fig. 4D).

Analysis of the data sets of four other mutants gave similar results as the NdhN-YFP mutant. Side-view classes showed the NDH-1 complex in the same two different positions, although the ratios differed somewhat. The YFP tag was partially present at a frequency between 5 and 25% (Table 1). It appeared at the center of the membrane domain for three mutants. In the NdhM-YFP mutant the tag appeared to be elongated in shape (Fig. 4F). A few particles had an extra large domain on top of the hydrophilic arm (Fig. 4H), as found for the NdhN-YFP mutant. The particles of NdhL-YFP mutant (Fig. 4I)

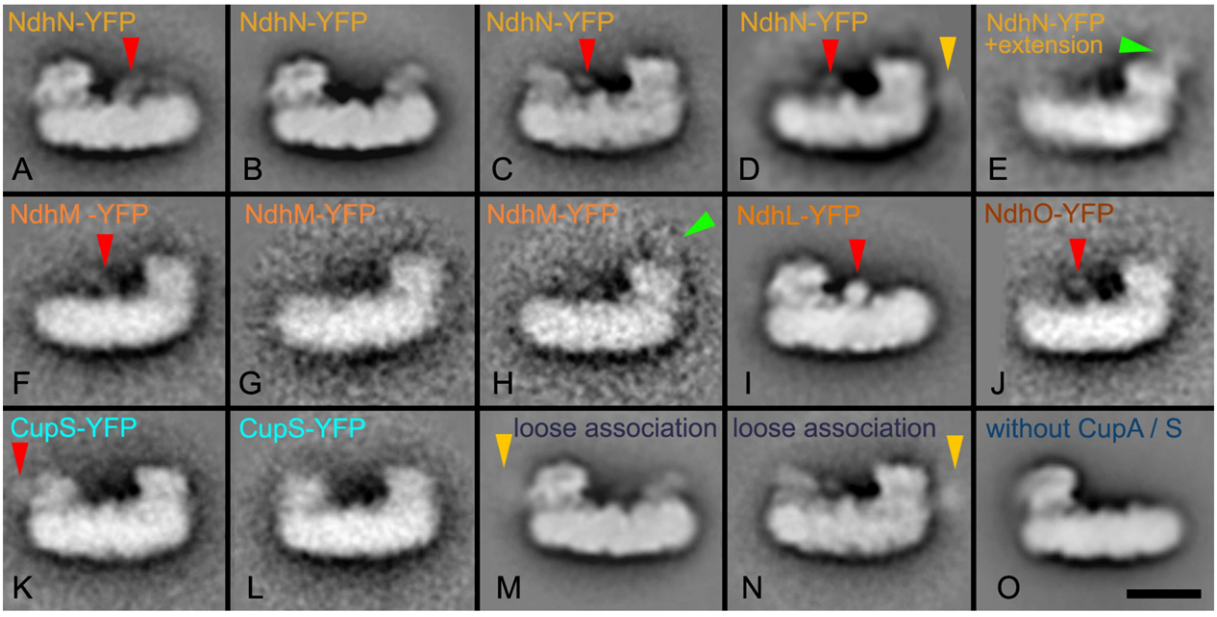

Fig. 4. Analysis of 2D projection maps from *Synechocystis* PCC 6803 NDH-1 particles in side view position. (A–E) 5 side-view classes from the NdhN-YFP mutant in two different handedness positions; (F–H) 3 classes from the NdhM-YFP mutant; (I) class of the NdhL-YFP mutant; (J) the NdhO-YFP mutant; (K,L) 2 main classes of the CupS mutant; (M,N) analysis of merged data sets from all mutants, splitted by handedness: subset of particles with a fuzzy mass shows a loosely associated mass next to the hydrophylic subdomain in both types of handedness (yellow arrowheads). This fuzzy mass is also seen in class D of the NdhN-YFP data set; (O) purified NDH-1, without CupA and CupS, reproduced from [24]. Notes: the position of YFP labels is indicated by red arrowheads. A green arrowhead indicates an extra density attached to the hydrophilic domain in subsets of particles from the NdhN-YFP and NdhM-YFP mutants. Scale bar for all frames equals 10 nm.

had the strongest appearance of the tag, but it was present only in 5–10% of the side views (Fig. 4I). In NdhO-YFP mutant the tag appeared to be elongated (Fig. 4J) and was in about the same position as NdhM-YFP (Fig. 4F). Finally, the CupS-YFP mutant was investigated (Fig. 4K, L) and showed to have the tag attached at the CupA domain, but at the outermost position of the NDH-1 complex (Fig. 4K). Besides the variation at the top of the hydrophilic domain (Fig. 4E,H), it appears that there is another loosely attached protein next to the hydrophilic domain (yellow arrowhead, Fig. 4D). This prompted us to have a closer look. Because this mass is not interfering with the position of the tags, all particles were pooled, classified and split in two sets with respect to their handedness. Both sets were classified and two subsets where this loosely attached density is visible are presented in Fig. 4M, N. Despite the fact that over 10,000 particles were compared, there was not one particular class where this extra mass appeared sharp. This indicates that this mass is not bound in a specific way.

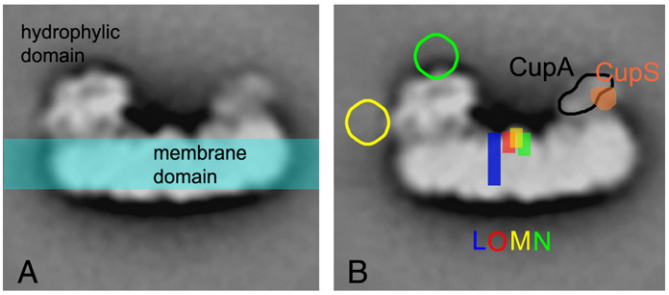

Fig. 5. Scheme for the determined subunit positions of NDH-1. (A) Two main domains of NDH-1 and the tentative position of the thylakoid membrane. (B) Schematic positions of the membrane spanning NdhL subunit (blue) and water-soluble subunits NdhO, NdhM and NdhN (marked red, yellow and green, respectively) and CupS (brown). The CupA (black line) is occupying the remainder of the protein domain at the tip of the membrane domain. Two loosely associated, unknown proteins are indicated by yellow and green circumferences.

4. Discussion

The aim of this work was two-fold. First, we wanted to investigate the unknown positions of the small subunits of cyanobacterial NDH-1 and second to demonstrate a fast and reliable way for subunit mapping by labeling them with tags of the GFP protein family and subsequent analysis by single particle electron microscopy.

Since NDH-1 complexes were isolated from the mutants using a Ni^{2+}-NTA column, all these complexes should have YFP-6His tag. However, the YFP tag appears to be present in only about 5–30% of the particles. The low percentage of labeled complexes (Table 1) may be explained that the labeled subunits were detached from the complex after affinity purification. However, this explanation may be not acceptable for the low percentage of NdhL-YFP containing complex because NdhL is a membrane subunit. Interestingly, the NdhL-YFP tag appears as the strongest of all tags (Fig. 4I).

While the YFP is in a non-overlapping position with the NDH-1 particles, it could be detected by the classification step of single particle EM and particles with or without a tag cluster in different classes, as was demonstrated for the set of particles from the NdhN-YFP mutant (Fig. 4A–D). The shape of the tag appeared after averaging to be circular (Fig. 4I) to rod-like, depending on the orientation (Fig. 4A,F,O), compatible with the rod-like β-barrel shape, as known form X-ray diffraction studies [32].

All the assigned small subunits (NdhL, M, N and O) were found to be associated to the membrane domain of NDH-1. This does not mean that they should be membrane integrated, because they could also be attached at the surface. Nevertheless, NdhL subunit has two putative membrane spanning helices, and is likely contributing to the membrane-integrated moiety of NDH-1. In earlier work, the position of NdhM, NdhN [11] and NdhL [12], was tentatively placed elsewhere. It is remarkable that NdhL, -N, -M, and -O are all localized in the middle of the membrane arm. We cannot provide an explanation for this, because the function of these proteins is not known. Likely the clustering is not a coincidence and we speculate that it has to do with a function that it is not present in the *E. coli* complex. Accidently, these subunits all locate at the site where in *Arabidopsis* mitochondrial complex I the unique carbonic anhydrase subunit domain is located [25]. Finally, it is not very surprising that the position of the CupS protein was found next to CupA at the tip of the membrane domain (Fig. 5).

The single particle analysis not only discriminates between particles with or without the YFP tag but also brings the variable presence of other densities in focus. In a previous study the CupA protein was found to be at the tip of the membrane domain, which gives the NDH-1 particles the U-shaped appearance. [22]. In most samples a mixture of U-shaped and L-shaped side view projections was found, which indicates the partial absence after purification of the labile CupA protein. Another interesting, but faint feature is an extra density next to the hydrophilic arm of NDH-1. It was noticed in one particular class of the NdhN-YFP mutant (Fig. 4D, yellow arrowhead). We pooled all particles in both orientations to see whether this feature gets sharper with a larger set of particles. Although it appears that in both groups there is a minority with this extension, it did not become sharp (Fig. 4M,N). This feature is not the result of proteins that lay coincidently next to NDH-1, but the fact that it is not sharp may indicate that it is bound in a flexible way. Another extension of the hydrophilic domain is seen at the top in a very small number of particles (green arrowhead, Fig. 4H). An obvious candidate would be “the missing protein” functioning in electron transport. However, no identity for such a protein is presently known.

Only one other labeling study with a GFP-fusion mutant was previously performed for a particular protein complex, the cardiac ryanodine receptor [27]. This study was, however, performed with crystallographic methods on two-dimensional crystals and no quantitation of the amount of bound label could be made. Because observed differences between WT and mutant were significant but quite small, it is possible that the label was not fully present, as it is the case in our NDH-1. To our knowledge no further EM investigations have been performed to determine subunit positions with the help of genetically introduced labels. In conclusion, the results on NDH-1 prove that a GFP/YFP tag can be revealed by single particle electron microscopy, after processing of data sets of moderate size, which can be collected within days by semi-automated data acquisition.

Table 1
Percentage of YFP-labeled particles per NDH-1 mutant, as estimated from the classification in single particle analysis.

Tagged NDH-1 subunit/gene	Number of particle projections analyzed	Total labeled (%)
NdhL	5000	5–10
NdhM	1755	25
NdhN	6714	30
NdhO	815	15
CupS	1050	25
Wild type	4400	No label used

Acknowledgement

This work was supported in part by the Academy of Finland (CoE project 118637).

References

[1] G.W. Tischendorf, H. Zeichhardt, G. Stöffler, Architecture of Escherichia-coli ribosome as determined by immune electron-microscopy, Proc. Natl. Acad. Sci. U. S. A. 72 (1975) 4820–4824.

[2] R.Y. Tsien, The green fluorescent protein, Annu. Rev. Biochem. 67 (1998) 509–544.
[3] J. Lippincott-Schwartz, E. Snapp, A. Kenworthy, Studying protein dynamics in living cells, Nat. Rev. Mol. Cell Biol. 2 (2001) 444–456.
[4] N.B. Cole, C.L. Smith, N. Sciaky, M. Terasaki, M. Edidin, J. Lippincott-Schwartz, Diffusional mobility of Golgi proteins in membranes of living cells, Science 273 (1996) 797–801.
[5] C.E.J. Dieteren, P.H.G.M. Willems, R.O. Vogel, H.G. Swarts, J. Fransen, R. Roepman, G. Crienen, J.A.M. Smeitink, L.G.J. Nijtmans, W.J.H. Koopman, Subunits of mitochondrial complex I exist as part of matrix- and membrane-associated subcomplexes in living cells, J. Biol. Chem. 283 (2008) 34753–34761.
[6] V. Zickermann, S. Kerscher, K. Zwicker, M.A. Tocilescu, M. Radermacher, U. Brandt, Architecture of complex I and its implications for electron transfer and proton pumping, Biochim. Biophys. Acta 1787 (2009) 574–583.
[7] T. Ogawa, H. Mi, Cyanobacterial NADPH dehydrogenase complexes, Photosynth. Res. 93 (2007) 69–77.
[8] F.R. Blattner, G. Plunkett, C.A. Bloch, N.T. Perna, V. Burland, M. Riley, J. Collado-Vides, J.D. Glasner, C.K. Rode, G.F. Mayhew, J. Gregor, N.W. Davis, H.A. Kirkpatrick, M.A. Goeden, D.J. Rose, B. Mau, Y. Shao, The complete genome sequence of Escherichia coli K-12, Science 277 (1997) 1453–1474.
[9] P. Hinchliffe, J. Carroll, L.A. Sazanov, Identification of a novel subunit of respiratory complex I from Thermus thermophilus, Biochemistry 45 (2006) 4413–4420.
[10] N. Battchikova, E.-M. Aro, Cyanobacterial NDH-1 complexes: multiplicity in function and subunit composition, Physiol. Plant. 131 (2007) 22–32.
[11] P. Prommeenate, A.M. Lennon, C. Markert, M. Hippler, P.J. Nixon, Subunit composition of NDH-1 complexes of Synechocystis sp. PCC 6803: identification of two new ndh gene products with nuclear-encoded homologues in the chloroplast Ndh complex, J. Biol. Chem. 279 (2004) 28165–28173.
[12] N. Battchikova, P. Zhang, S. Rudd, T. Ogawa, E.-M. Aro, Identification of NdhL and Ssl1690 (NdhO) in NDH-1L and NDH-1M complexes of *Synechocystis* sp. PCC 6803, J. Biol. Chem. 280 (2005) 2587–2595.
[13] D. Rumeau, N. Becuwe-Linka, A. Beyly, M. Louwagie, J. Garin, G. Peltier, New subunits NDH-M, -N, and -O, encoded by nuclear genes, are essential for plastid ndh complex functioning in higher plants, Plant Cell 17 (2005) 219–232.
[14] H. Shimizu, L. Peng, F. Myouga, R. Motohashi, K. Shinozaki, T. Shikanai, CRR23/NdhL is a subunit of the chloroplast NAD(P)H dehydrogenase complex in Arabidopsis, Plant Cell Physiol. 49 (2008) 835–842.
[15] A. Takabayashi, N. Ishikawa, T. Obayashi, S. Ishida, J. Obokata, T. Endo, F. Sato, Three novel subunits of Arabidopsis chloroplastic NAD(P)H dehydrogenase identified by bioinformatic and reverse genetic approaches, Plant J. 57 (2009) 207–219.
[16] S. Yabuta, K. Ifuku, A. Takabayashi, S. Ishihara, K. Ido, N. Ishikawa, T. Endo, F. Sato, Three PsbQ-Like Proteins Are Required for the Function of the Chloroplast NAD(P)H Dehydrogenase Complex in Arabidopsis, Plant Cell Physiol. 51 (2010) 866–876.
[17] M. Suorsa, S. Sirpiö, V. Paakkarinen, N. Kumari, M. Holmström, E.M. Aro, Two proteins homologous to PsbQ are novel subunits of the chloroplast NAD(P)H Dehydrogenase, Plant Cell Physiol. 51 (2010) 877–883.
[18] S. Sirpiö, Y. Allahverdiyeva, M. Holmstrom, A. Khrouchtchova, A. Haldrup, N. Battchikova, E.M. Aro, Novel nuclear-encoded subunits of the chloroplast NAD(P)H dehydrogenase complex, J. Biol. Chem. 284 (2009) 905–912.
[19] M. Shibata, H. Ohkawa, T. Kaneko, H. Fukuzawa, S. Tabata, A. Kaplan, T. Ogawa, Distinct constitutive and low CO_2-induced CO_2 uptake systems in cyanobacteria: genes involved and their phylogenetic relationship with homologous genes in other organisms, Proc. Natl. Acad. Sci. U. S. A. 98 (2001) 11789–11794.
[20] P. Zhang, N. Battchikova, T. Jansen, J.T. Appel, T. Ogawa, E.M. Aro, Expression and functional roles of the two distinct NDH-1 complexes and the carbon acquisition complex NdhD3/NdhF3/CupA/Sll1735 in *Synechocystis* sp PCC 6803, Plant Cell 16 (2004) 3326–3340.
[21] P. Zhang, N. Battchikova, N. Paakkarinen, H. Katoh, M. Iwai, M. Ikeuchi, H.B. Pakrasi, T. Ogawa, E.M. Aro, Isolation, subunit composition and interaction of the NDH1 complexes from Thermosynechococcus elongatus BP1, Biochem. J. 390 (2005) 513–520.
[22] L.A. Sazanov, P. Hinchliffe, Structure of the hydrophilic domain of respiratory complex I from Thermus thermophilus, Science 311 (2006) 1430–1436.
[23] T. Clason, T. Ruiz, H. Schägger, G. Peng, V. Zickermann, U. Brandt, H. Michel, M. Radermacher, The structure of eukaryotic and prokaryotic complex I, J. Struct. Biol. 169 (2010) 81–88.
[24] A.A. Arteni, P. Zhang, N. Battchikova, T. Ogawa, E.-M. Aro, E.J. Boekema, Structural characterization of NDH-1 complexes of *Thermosynechococcus elongatus* by single particle electron microscopy, Biochim. Biophys. Acta 1757 (2006) 1469–1475.
[25] S. Sunderhaus, N. Dudkina, L. Jänsch, J. Klodmann, J. Heinemeyer, M. Perales, E. Zabaleta, E. Boekema, H.P. Braun, Carbonic anhydrase subunits form a matrix-exposed domain attached to the membrane arm of mitochondrial complex I in plants, J. Biol. Chem. 281 (2006) 6482–6488.
[26] X. Zhang, E. Settembre, C. Xu, P.R. Dormitzer, R. Bellamy, S.C. Harrison, N. Grigorieff, Near-atomic resolution using electron cryomicroscopy and single-particle reconstruction, Proc. Natl. Acad. Sci. U. S. A. 105 (2008) 1867–1872.
[27] P.J. Jones, X. Meng, B. Xiao, S. Cai, J. Bolstad, T. Wagenkencht, Z. Liu, Localization of PKA phosphorylation site, Ser2030, in the three-dimensional structure of cardiac ryanodine receptor, Biochem. J. 410 (2008) 261–270.
[28] I.M. Folea, P. Zhang, M.M. Nowaczyk, T. Ogawa, E.M. Aro, E.J. Boekema, Single particle analysis of thylakoid proteins from Thermosynechococcus elongatus and Synechocystis 6803: localization of the CupA subunit of NDH-1, FEBS Lett. 582 (2008) 249–254.
[29] I. Wittig, M. Karas, H. Schägger, High resolution clear native electrophoresis for in-gel functional analysis and fluorescence studies of membrane protein complexes, Mol. Cell. Proteomics 6 (2007) 1215–1225.
[30] G.T. Oostergetel, W. Keegstra, A. Brisson, Automation of specimen selection and data acquisition for protein electron crystallography, Ultramicroscopy 74 (1998) 47–59.
[31] I.M. Folea, P. Zhang, E.M. Aro, E.J. Boekema, Domain organization of photosystem II in membranes of the cyanobacterium Synechocystis PCC6803 investigated by electron microscopy, FEBS Lett. 582 (2008) 1749–1754.
[32] F. Yang, L.G. Moss, G.N. Phillips, The molecular structure of green fluorescent protein, Nat. Biotechnol. 14 (1996) 1246–1251.